J Mater Sci (2009) 44:1969–1976
DOI 10.1007/s10853-009-3297-y

Developing aluminium–zinc-based a new alloy for tribological applications

Temel Savaşkan · Osman Bican · Yasin Alemdağ

Received: 9 October 2008 / Accepted: 26 January 2009 / Published online: 26 February 2009

Abstract In order to develop aluminium–zinc-based a new alloy for tribological applications, six binary Al–Zn and seven ternary Al–25Zn–(1–5)Cu were prepared by permanent mould casting. Their microstructure and mechanical properties were investigated. Dry sliding friction and wear properties of the ternary alloys were investigated using a pin-on-disc machine. Surface and subsurface regions of the wear samples were studied with scanning electron microscopy (SEM). The highest hardness and tensile strength were obtained with the Al–25Zn alloy among the binary ones. The microstructure of this alloy consisted of aluminium-rich α and eutectoid $\alpha + \eta$ phases. Addition of copper to this alloy resulted in the formation of θ ($CuAl_2$) phase. The hardness of the ternary alloys increased with increasing copper content. The highest tensile and compressive strengths and wear resistance and the lowest friction coefficient were obtained from the ternary Al–25Zn–3Cu alloy. The dimensional change measured on ageing (stabilization) of this alloy was found to be much lower than that obtained from the copper containing zinc-based alloys. Microstructural changes were observed below the surface of the wear samples of the Al–25Zn–3Cu alloy. These changes were related to the heavy deformation of the surface material due to normal and frictional forces, and smearing and oxidation of wear material. Adhesion was found to be the main wear mechanism for the alloys tested.

T. Savaşkan (✉) · O. Bican · Y. Alemdağ
Mechanical Engineering Department, Karadeniz Technical University, Kanuni Campus, 61080 Trabzon, Turkey
e-mail: savaskan@ktu.edu.tr

Introduction

Zinc-based ternary and quaternary alloys have been proven to be good bearing materials [1–5]. Their wear resistance was found to be considerably higher than that obtained from the traditional bearing materials including bronze and cast iron [5–8]. However, the copper containing zinc-based ternary and quaternary alloys suffer from dimensional instability and low ductility problems [5–11]. The instability problem arises mainly due to the transformation of metastable ε ($CuZn_4$) phase into the stable T′ (Al_4Cu_3Zn) and η phases by a four phase reaction $(\varepsilon + \alpha \rightleftharpoons T' + \eta)$ and the low ductility was related to the brittleness of zinc and copper-rich phases [3, 9–11]. To eliminate or minimise these problems zinc was replaced with aluminium in these alloys and this resulted in the formation of stable θ ($CuAl_2$) particles instead of metastable ε phase [7, 12]. As a result of these investigations, Al–40Zn–3Cu and Al–40Zn–3Cu–2Si alloys have been developed [7, 12]. These alloys exhibited almost the same specific strength as the zinc-based monotectoid alloys, but their elongation to fracture was found to be much higher than those of the latter [7, 8, 12–18]. As observed with the zinc-based monotectoid alloys, the wear resistance of these alloys was also found to be much higher than that of a traditional bearing bronze [7, 12]. This indicates that the zinc-based bearing alloys can be replaced successfully with the aluminium-based alloys containing zinc, copper and/or silicon for tribological applications. However, the effects of zinc content on the mechanical and tribological properties of aluminium-based alloys have not been investigated. In order to develop aluminium-based new alloys with desirable properties the most suitable zinc content should be determined. For this reason the best composition for the base alloy (binary Al–Zn) should be determined first. Then the ternary or

quaternary alloys can be designed and produced by the addition of copper or silicon to the base alloy. Therefore, the main aim of this work was to design and produce aluminium–zinc-based new ternary alloys with desirable mechanical and wear properties.

Experimental procedure

Preparation of alloys, chemical composition and microstructure

Six binary Al–Zn, seven ternary Al–25Zn–(1–5)Cu were prepared from commercially pure aluminium (99.7%), high purity zinc (99.9%) and electrolytic copper (99.9%). Alloys were melted in an electric furnace at a temperature of 680 °C and poured into a steel mould at room temperature. The mould had a conical shape with a length of 180 mm, a bottom diameter of 57 mm and a top diameter of 70 mm.

The chemical compositions of the alloys were determined by atomic absorption analysis method. Samples for microstructural examinations were prepared using standard metallographic techniques, etched with 3% NaOH solution in alcohol and examined by optical and scanning electron microscopy (SEM).

Physical and mechanical tests

The density of the alloys was determined by measuring their volume and mass. The Brinell hardness of the alloys was measured using a load of 62.5 kgf and a 2.5 mm steel ball as indenter. The tensile and compressive strengths of the alloys were measured using round specimens with a dimension (diameter × gauge length) 8 mm × 40 mm and 10 mm × 10 mm, respectively at a strain rate of 5.9×10^{-3} s^{-1}. Vicker's micro-hardness measurements were made on the metallographic and wear samples at a load of 20 gf. The dimensional stability of the alloy (Al–25Zn–3Cu), which showed the highest tensile and compressive strengths, was monitored at 150 °C for 100 h using round specimens having the dimensions of 8 × 45 mm^2. A bench micrometer with an accuracy of ±0.003 mm was used to measure the length of the specimens. At least, three readings were taken to determine the density, hardness, microhardness, tensile and compressive strengths, elongation to fracture and the dimensional changes of the alloys.

Friction and wear tests

The friction and wear tests were carried out using a pin-on-disc machine. A schematic diagram of this machine is shown in Fig. 1. The machine consists of a disc, a pin (specimen), and its mounting system, a loading system, and friction force and a temperature measurement system. The disc was made of SAE 1045 steel (0.42%–0.50% C, 0.5%–0.8% Mn, 0.035% P, 0.03% S and balance Fe) with a diameter of 200 mm and a hardness of 50 ± 1 HRC. Specimens with a size of 10 × 15 × 25 mm^3 were prepared from the alloys. Friction and wear tests were performed under a constant pressure of 1.5 MPa and a sliding speed of 1 ms^{-1}. The friction force was determined using a S-50 type load cell and the coefficient of friction of the alloys calculated by dividing friction force by the normal load. The friction and wear tests were carried out for a sliding distance of 2500 m. The temperatures of the wear samples were monitored by inserting a copper–nickel

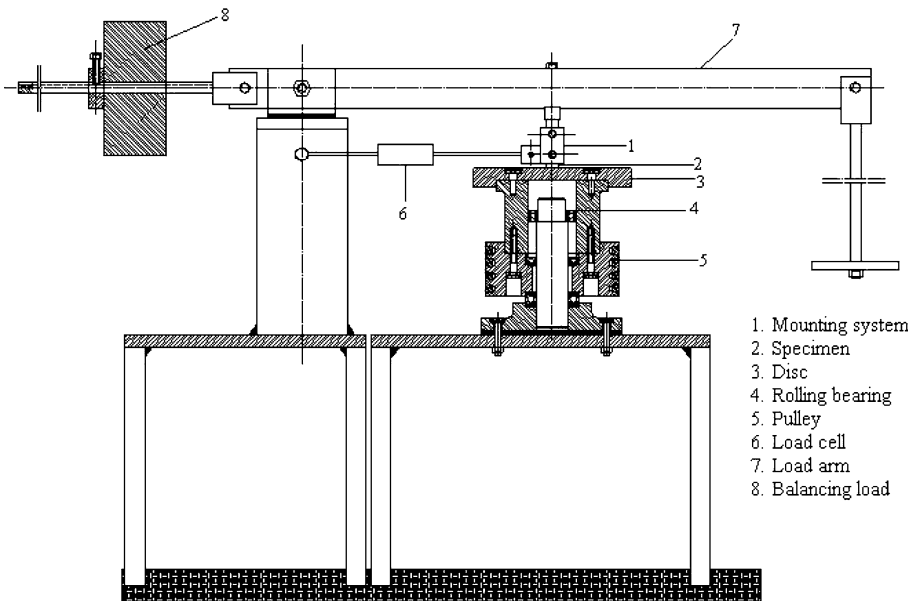

Fig. 1 A schematic diagram of the test machine

thermocouple in a hole at a distance of 1.5 mm from the rubbing surface. Each specimen was ultrasonically cleaned and weighed before wear tests using a balance with an accuracy of 0.01 mg. The disc was cleaned with organic solvents to remove surface contaminants before each test. The wear samples were removed after every sliding distance of 500 m, cleaned in solvents and weighed to determine the mass loss. This procedure was repeated for a total sliding distance of 2500 m. The measured values of mass loss for all the specimens tested were converted into volume loss using the measured density of the alloys. The surface and subsurface of the wear samples were examined using SEM.

Results

Chemical composition and microstructure

The chemical compositions of the aluminium-based alloys produced are given in Table 1. The microstructure of the binary Al–25Zn alloy consisted of aluminium rich α dendrites and eutectoid $\alpha+\eta$ phases, Fig. 2a. Addition of copper to this alloy produced inter-metallic θ particles mainly in the inter-dendritic regions, Fig. 2b–d. It was observed that as the copper content of the ternary alloys increased the number and the size of these particles increased.

Physical and mechanical test results

The change of the density, hardness, tensile strength and percentage elongation to fracture of the binary Al–Zn alloys as a function of zinc content are shown in Fig. 3. It can be seen from this figure that the hardness and tensile strength of the binary alloys increased with increasing zinc content up to 25%, above which the trend reversed. This indicates that the Al–25Zn alloy has the highest hardness and tensile strength among the binary ones. However, their elongation to fracture decreased with increasing zinc content up to 30%, above which it showed a small increase. It was also observed that the density of the binary alloys increased almost linearly with increasing zinc content.

Table 1 The chemical compositions of the aluminium-based alloys

Alloy	Chemical composition (wt%)		
	Al	Zn	Cu
Al–10Zn	90.6	9.4	–
Al–20Zn	81.2	18.8	–
Al–25Zn	74.8	25.2	–
Al–30Zn	71.3	28.7	–
Al–40Zn	61.2	38.8	–
Al–50Zn	48.6	51.4	–
Al–25Zn–1Cu	74.0	25.1	0.9
Al–25Zn–2Cu	72.6	25.2	2.2
Al–25Zn–2.5Cu	72.3	25.1	2.6
Al–25Zn–3Cu	71.7	25.2	3.1
Al–25Zn–3.5Cu	71.1	25.2	3.7
Al–25Zn–4Cu	70.5	25.3	4.2
Al–25Zn–5Cu	69.9	25.2	4.9

The variation of the density, hardness, micro-hardness of α phase, tensile and compressive strengths and percentage elongation to fracture with copper content of the ternary Al–25Zn–(1–5)Cu alloys are shown in Fig. 4. This figure shows that the density and the hardness of the ternary alloys increase, but their elongation to fracture decreases continuously with increasing copper content. The tensile and compressive strengths of the alloys increased with increasing copper content up to 3% Cu, above which the trend reversed. The micro-hardness of the α phase of the alloys also increased with increasing copper content up to 3%, but it became almost constant above this level. These observations indicate that the Al–25Zn–3Cu alloy has the highest tensile and compressive strengths among ternary alloys containing copper.

Figure 5 shows the changes in hardness and length of the Al–25Zn–3Cu alloy as a function of ageing time. It can be seen that the length of the alloy samples increased, but their hardness decreased on ageing for the first 10 h period, after which both parameters became almost constant. The maximum amount of increase observed in the length of this alloy was found to be approximately 0.03%.

Friction and wear test results

The friction coefficient, temperature and wear loss (wear volume) versus sliding distance curves for the ternary alloys are shown in Figs. 6, 7, 8, respectively. The friction coefficient and the temperature of the alloys showed a sharp increase during the initial period of the test run and reached almost constant levels after a sliding distance of approximately 200 m. However, their wear volume increased almost linearly with increasing sliding distance.

The change of friction coefficient, temperature and wear volume as a function of copper content of the ternary alloys are shown in Fig. 9. It can be seen that the friction coefficient, temperature and wear volume of the alloys decrease with increasing copper content up to 3%, above which the trend reverses.

The wear surfaces of the alloys were characterised by smearing and fine scratches, Fig. 10a–c. However, smearing was observed to be the dominant wear mechanism for the alloys tested. Two distinct layers were observed below the surface of the wear samples of Al–25Zn–3Cu alloy tested for a sliding distance of 2500 m, Fig. 11. These

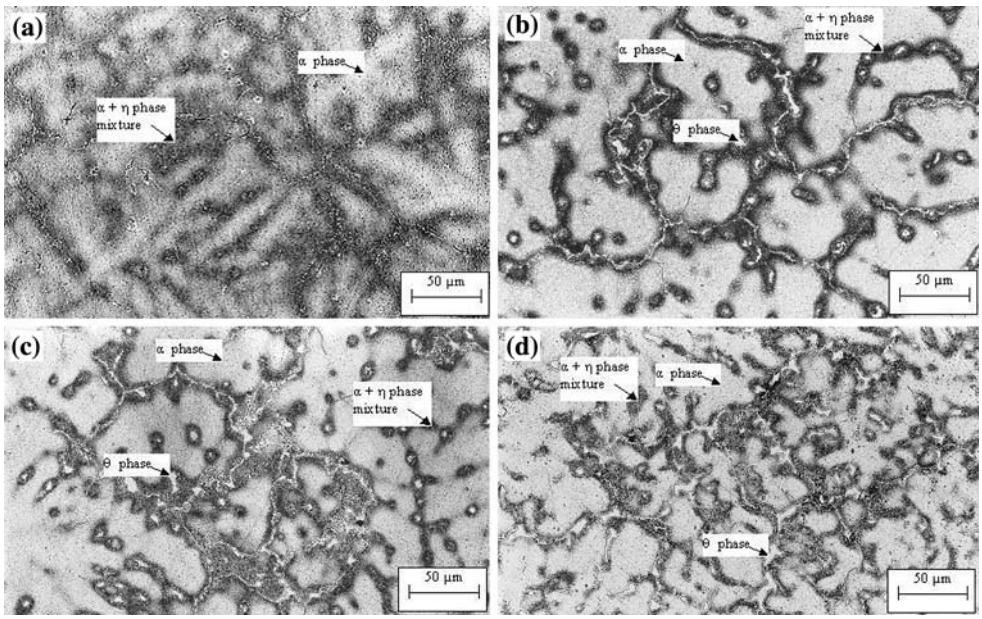

Fig. 2 Microstructures of **a** Al–25Zn, **b** Al–25Zn–1Cu, **c** Al–25Zn–3Cu, **d** Al–25Zn–5Cu alloys

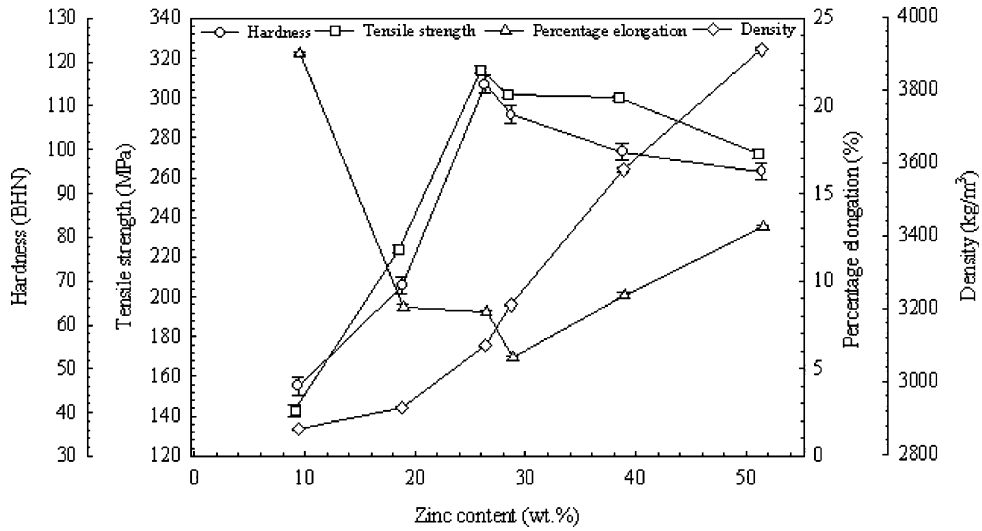

Fig. 3 The variation of the hardness, tensile strength, percentage elongation to fracture and density of the binary Al–Zn based alloys with zinc content

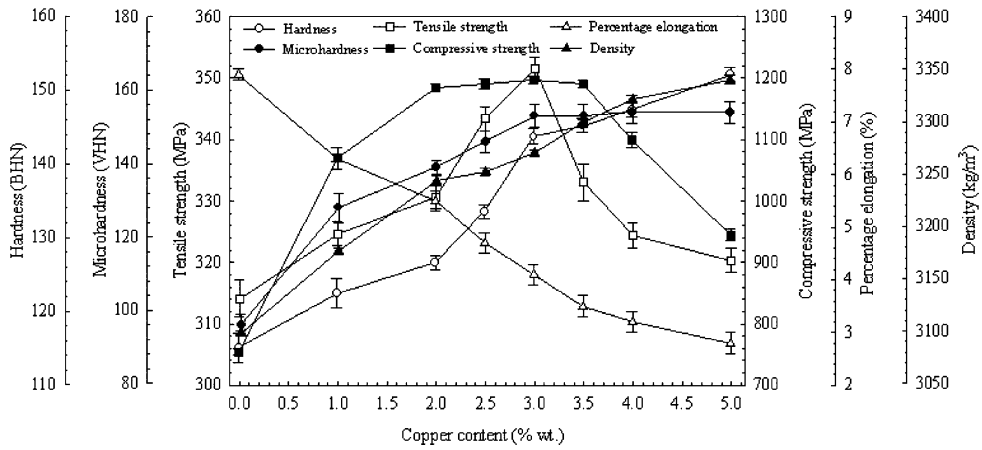

Fig. 4 The change in hardness, micro-hardness of α phase, tensile and compressive strength and percentage elongation to fracture of the binary and ternary alloys with copper content

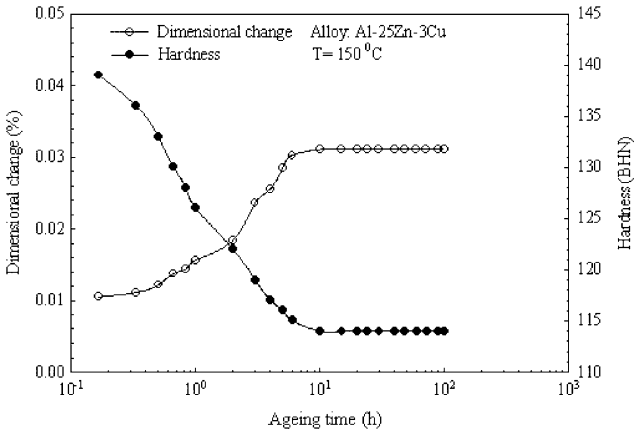

Fig. 5 The variation of the hardness and dimensional change with ageing time

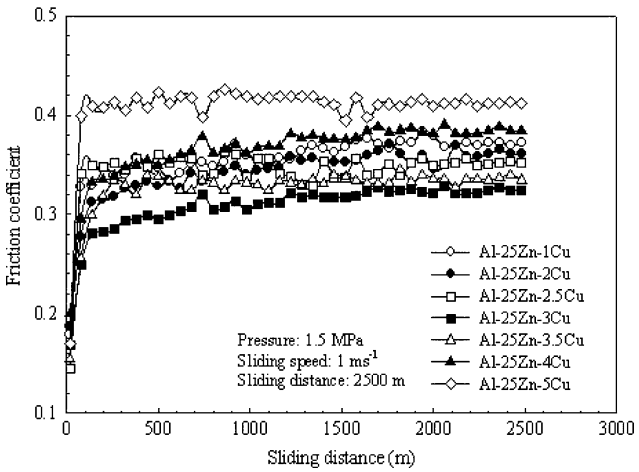

Fig. 6 The variation of coefficient versus sliding distance for the alloys tested

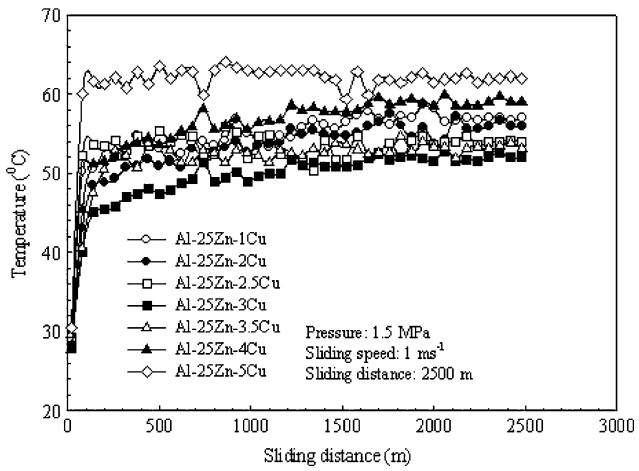

Fig. 7 The change of temperature as a function of sliding distance for the ternary alloys

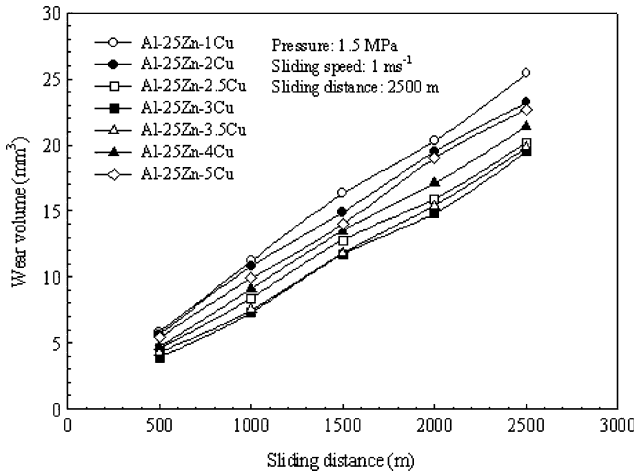

Fig. 8 The volume loss due to wear obtained from tested alloys versus sliding distance

layers were marked as A and B starting from the rubbing surface. The layer A has a fine-grained microstructure, while the layer B shows flow lines oriented in the sliding direction. The change of micro-hardness as a function of depth from the surface of a wear sample is shown in Fig. 12. It can be seen that the micro-hardness of the sample shows a sharp decrease with increasing depth in layer A and reaches almost a constant level after dropping to its lowest value in layer B and becoming almost constant after showing a gradual increase. This indicates that the layer A has the highest, but the layer B has the lowest micro-hardness values. However, the final level of the micro-hardness was observed to be approximately the same as the value obtained from the α phase of the original alloy microstructure.

Discussion

The microstructure of the Al–25Zn binary alloy consisted of aluminium-rich α dendrites, eutectoid $\alpha + \eta$ phase mixture, Fig. 2a. Copper addition to this alloy resulted in the formation of θ inter-metallic phase mainly in the inter-dendritic regions. The size and the number of this inter-metallic phase in the ternary alloys increased as the copper content increased, Fig. 2b–d. These observations are in agreement with the results obtained from the Al–40Zn-based ternary alloys containing copper [7, 12].

The maximum increase (0.03%) in the length of the Al–25Zn-–3Cu alloy on ageing was found to be much lower than that (>0.2%) obtained from the copper containing zinc-based alloys [5]. This can be related to the formation of stable intermetallic θ phase in the former instead of metastable ε phase [5].

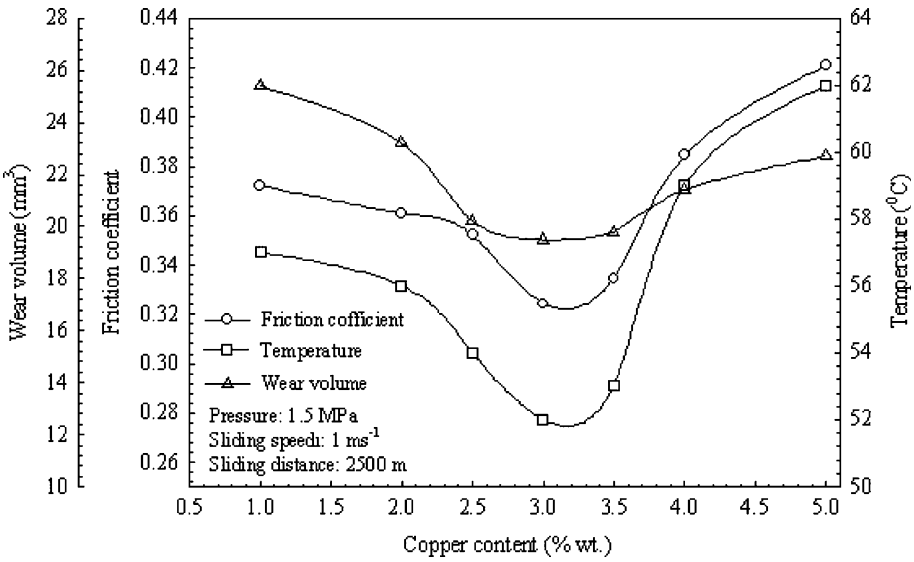

Fig. 9 The change of the friction coefficient, temperature and wear volume of the alloys tested versus copper content

Among the binary Al–Zn alloys the maximum hardness and tensile strength were obtained with the Al–25Zn alloy, Fig. 3. This may be related to the solid solution hardening mechanism [19]. According to the binary Al–Zn phase diagram the solid solubility of zinc in aluminium reaches a maximum at approximately 25% Zn at the eutectoid temperature [20–22]. Since the hardness and strength of solid solutions increases with the amount of solubility the maximum hardness and tensile strength are expected with the Al–25Zn alloy in the binary Al–Zn system. This observation is in a good agreement with the results of previous investigations carried out mainly on the decomposition behaviour of the binary Al–Zn alloys [20–22].

The hardness of the Al–25Zn-based ternary alloys increased, but their elongation to fracture decreased almost continuously as the copper content increased, Fig. 4. However, their tensile and compressive strengths and the micro-hardness of the α phase increased with increasing copper content up to 3%, above which the trend reversed for the first two properties, but the latter became almost constant. These observations can be explained in terms of solid solution hardening mechanism and microstructural details. As explained in previous papers [7, 12, 14] the α phase of the Al–Zn–Cu alloys becomes saturated with copper when their copper content reaches approximately 3%. It is also known that addition of copper to Al–Zn alloys results in the formation of hard and brittle θ phase [7, 12, 14]. These facts explain why the tensile and compressive strengths and the micro-hardness of the α phase of the ternary alloys reach their maximum values at 3% Cu, while their hardness increases almost continuously with increasing copper content. The decrease in the elongation to fracture may be related to the presence and distribution of the θ phase. Metallographic examinations showed that the particles of this intermetallic phase were formed mainly in the inter-dendritic regions of the ternary alloys, Fig. 2b–d. These particles may reduce the elongation to fracture by weakening the bonding between the dendrites or causing brittleness in the inter-dendritic regions of the alloys.

The friction coefficients of the alloys showed a sharp increase during the initial period of the test and reached almost constant levels after 200 m sliding distance Fig. 6. Their temperatures showed a very similar trend, Fig. 7. These observations may be related to the smoothing out of the wear surfaces due to the wear-in process and formation of oxide films on these surfaces as explained in the previous papers [7, 12, 23–26].

The wear resistance of the copper containing Al–25Zn-based ternary alloys increased with copper content up to 3%, above which the trend reversed, Fig. 9. This may be explained in terms of solid solubility of copper in aluminium and the mechanical properties of the alloys. The tensile and compressive strengths of the Al–25Zn-based ternary alloys reach their ultimate level at 3% Cu due to the reasons given above. According to the adhesive wear theory and previous wear results obtained from similar alloys the wear loss is inversely proportional to the hardness, especially micro-hardness of the matrix and tensile strength of the materials [7, 8, 12–15]. Therefore, the highest wear resistance can be expected from the ternary alloy containing 3% Cu.

Wear surfaces of the Al–25Zn-based alloys were characterised by smearing and scratches, Fig. 10a–c. As explained in previous papers smearing occurs due to removal and back-transfer of wear material from disc to the sample surface, while the scratches were produced by the ploughing action of the hard intermetallic particles during their removal from the sample surface [23–27].

Metallographic examinations revealed two distinct layers below the surface of the wear samples of Al–25Zn–3Cu

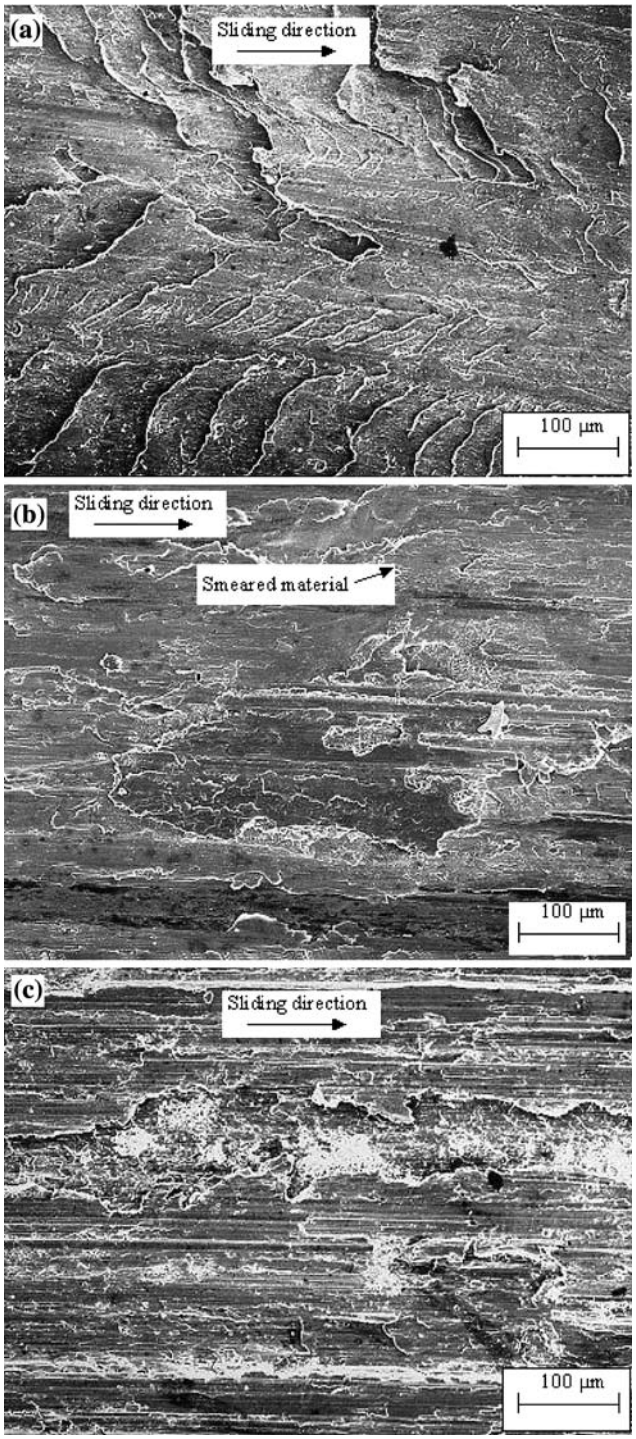

Fig. 10 Wear surfaces of **a** Al–25Zn–1Cu, **b** Al–25Zn–3Cu **c** Al–25Zn–5Cu alloys

alloy. These were marked as layer A and layer B, Fig. 11. The layer A had a fine-grained microstructure, while the layer B revealed flow lines oriented in the sliding direction. Micro-hardness profile obtained from the longitudinal section of the wear samples showed that the layer A is harder, but the layer B is softer than the original alloy,

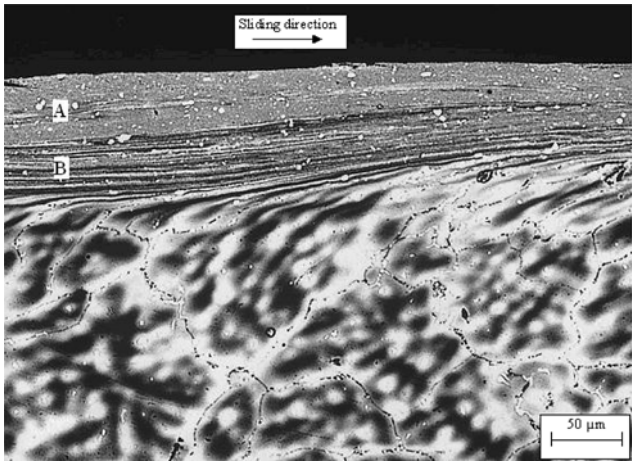

Fig. 11 The cross-sectional view of a wear sample of the Al–25Zn–3Cu alloy

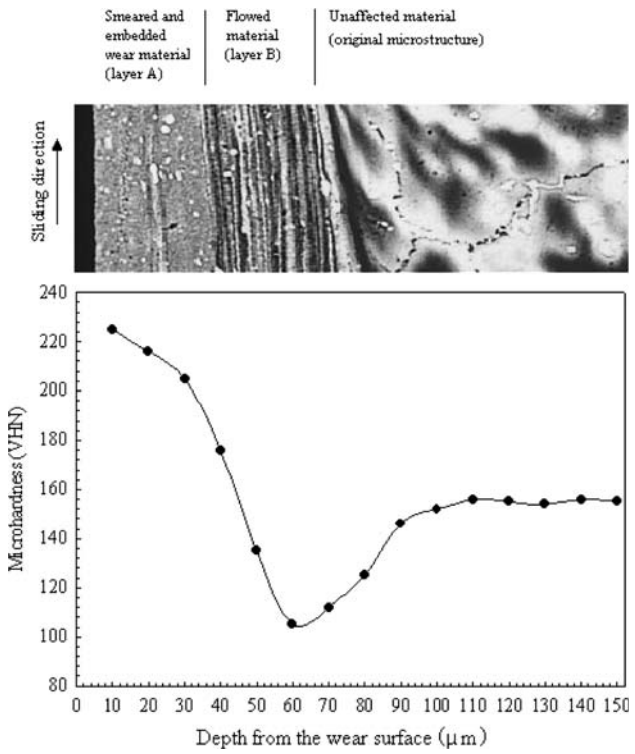

Fig. 12 The variation of micro-hardness as a function of depth from the surface of a wear sample of the Al–25Zn–3Cu alloy

Fig. 12. These observations suggest that the former is a mechanically mixed layer (MML) which was produced by the smearing of the wear material on the surface, while the layer B formed as result of heavy plastic deformation of the surface material. The high hardness of the layer A may be attributed to the heavy deformation and oxidation of the wear material, while the low hardness of the layer B may be related to either deformation and recrystallization or decomposition of metastable phases and coarsening of the

transformation products in the wear sample during testing [27–33]. However, formation of flow lines in the layer B may be attributed to the combined effect of frictional force and the maximum shear stress which takes place at the surface of the sample under dry sliding condition [27–33]. It is probable that in early stages of the test the layer B forms first due to heavy plastic deformation and then the layer A starts to form by smearing of the wear products back transferred from the disc to the sample surface [24–33].

Conclusion

1. The highest hardness and tensile strength were obtained with the Al–25Zn alloy among the aluminium-based binary alloys.
2. The microstructure of the Al–25Zn–(1–5)Cu alloys consisted of aluminium-rich α, eutectoid $\alpha + \eta$ and θ phases.
3. The tensile and compressive strengths of the Al–25Zn–(1–5)Cu alloys increased with increasing copper content up to 3%, above which the trend reversed.
4. The Al–25Zn–3Cu alloy exhibited much lower expansion on ageing than that observed with the zinc-based alloys. This indicates that this alloy is much more stable than the zinc-based alloys containing aluminium and copper.
5. The highest wear resistance was obtained with the Al–25Zn–3Cu alloy among the ones tested.
6. The wear resistance of the alloys tested was found to be dependent upon their tensile and compressive strengths rather than their hardness.
7. Microstructural changes were observed below surface of the wear samples of the Al–25Zn–3Cu alloy. They appeared to be a fine-grained layer and a heavily deformed region oriented in the sliding direction. Formation of these layers was related to heavy deformation of surface material and smearing of wear debris due to high pressure and frictional force.
8. Wear surfaces of the Al–25Zn–Cu alloys were characterised by smearing and scratches, but smearing appeared to be dominant mechanism for their wear.

Acknowledgement This work was funded by the Scientific and Technological Research Council of Turkey (TUBITAK). Grant No: 108M292.

References

1. Gebhardt E (1941) Z Metallkd 33:297
2. Köster W, Moeller K (1942) Z Metallkd 34:206
3. Lohberg K (1983) Z Metallkd 74:456
4. Murphy S, Savaşkan T (1984) Wear 98:151
5. Savaşkan T, Murphy S (1987) Wear 116:211
6. Lee P, Savaşkan T, Laufer E (1987) Wear 117:79
7. Alemdağ Y, Savaşkan T (2008) Tribol Lett 29:221
8. Savaşkan T, Bican O (2005) Mater Sci Eng A 404:259
9. Murphy S (1980) Z Metallkd 71:96
10. Yaohua Z, Murphy S (1986) Chin J Met Sci Technol 2:105
11. Yaohua Z (1989) Chin J Met Sci Technol 5:113
12. Alemdağ Y, Savaşkan T (2009) Tribol Int 42:176
13. Prasad BK (1997) Mater Trans JIM 38:701
14. Savaşkan T, Hekimoğlu AP, Pürçek G (2004) Tribol Int 37:45
15. Azaklı Z, Savaşkan T (2008) Tribol Int 41:9
16. Prasad BK, Patwardhan AK, Yegneswaran AH (1997) Mater Trans JIM 38:701
17. Prasad BK, Patwardhan AK, Yegneswaran AH (1996) Wear 199:142
18. Pandey JP, Prasad BK (1997) Z Metallkd 88:739
19. Ashby MF, Jones DRH (1983) Engineering materials. Pergamon Press, England
20. Rao KK, Herman H (1966) J Inst Met 94:420
21. Anantharaman TR, Ramaswamy V, Butler EP (1974) J Mater Sci 9:240. doi:10.1007/BF00550947
22. Anantharaman TR, Satyanarayana KG (1973) Scr Metal 7:189
23. An J, Liu YB, Lu Y (2004) Mater Sci Eng A 373:294
24. Rodriguez J, Poza P, Garrido MA et al (2007) Wear 262:292
25. Pürçek G, Savaşkan T, Küçükömeroğlu T et al (2002) Wear 252:894
26. Geng H, Ma J (1993) Wear 169:201
27. Şahin Y, Murphy S (1998) Wear 214:98
28. Iwai Y, Hou W, Honda T et al (1996) Wear 196:46
29. Prasad BK (2007) Wear 262:262
30. Akarca SS, Altenhof WJ, Alpas AT (2007) Tribol Int 40:735
31. Prasada Rao AK, Das K, Murty BS et al (2008) Wear 264:638
32. Chen CM, Yang CC, Chao CG (2005) Mater Sci Eng A 397:178
33. Modia OP, Rathoda S, Prasada BK et al (2007) Tribol Int 40:1137